Mechanics of Materials 9 (1990) 65–80
Elsevier

OBSERVATIONS ON STRESS–FORCE–FABRIC RELATIONSHIPS IN IDEALIZED GRANULAR MATERIALS

Richard J. BATHURST * and Leo ROTHENBURG

Civil Engineering Department, University of Waterloo, Waterloo, Ontario, Canada N2L 3G1

Received 26 June 1989; revised version received 11 December 1989

The paper presents a series of theoretical developments and numerical experiments directed at quantifying important features of the micromechanical behavior of granular media by introducing *average* characteristics of fabric anisotropy and certain statistical averages of contact forces. The introduced characteristics are explicitly linked to stress through a stress–force–fabric relationship. Numerical simulations are used to verify this relationship for plane assemblies and to trace the evolution of induced anisotropy in contact orientations and contact forces. It is shown that at large strain the degree of anisotropy in contact orientations achieves some limiting value and the macroscopic angle of friction at large strains can be expressed directly in terms of this value. Effects of the angle of interparticle friction and magnitude of interparticle stiffness on the shear capacity of numerical assemblies at large strain are investigated.

Nomenclature

a_{ij}	coefficients of contact normal anisotropy
a	second-order coefficient of contact normal anisotropy (plane systems) ($a \rightarrow a_\infty$ at steady-state)
a_n	second-order coefficient of average normal force anisotropy (plane systems)
a_ω, a_t	second-order coefficients of average tangential force anisotropy (plane systems)
A	$(a_n + a_t)/a$
b	fourth-order coefficient of contact normal anisotropy (plane systems)
$E(\theta)$, $E(\boldsymbol{n})$	contact normal distribution function
$\boldsymbol{f}^c$, $\boldsymbol{f}_n^c$, $\boldsymbol{f}_t^c$	contact force vector, normal and tangential (shear) contact force vector components
$\bar{f}_n(\theta)$, $\bar{f}_t(\theta)$	distribution of average normal and tangential (shear) contact forces
$\bar{f}_0$	average normal contact force
$\mathbf{l}^c$, l^c	contact vector, contact vector length = distance between centre of particle and surface contact
$\bar{l}(\theta)$	distribution of average contact length orientations
$\bar{l}_0$	assembly average contact vector length
k_n, k_t	normal and tangential contact stiffnesses
m_v	M/V, contact density
M	total number of assembly contacts
$\boldsymbol{n}$	unit vector
$\boldsymbol{n}^c$	contact normal vector
N	total number of assembly particles
$\boldsymbol{N}$	symmetric second-order average normal force tensor
$\boldsymbol{t}^c$	contact tangent vector
$\bar{r}_0$	average particle radius
$\boldsymbol{R}$	symmetric second-order fabric tensor
$\boldsymbol{T}$	symmetric second-order deviator average tangential force tensor

* Permanent address: Civil Engineering Department, Royal Military College of Canada, Kingston, Ontario, Canada K7K 5L0.

V	assembly area (or volume)
ϵ_v	$\epsilon_{11}+\epsilon_{22}$, volumetric strain
ϵ_t	$\sqrt{(\epsilon_{11}-\epsilon_{22})^2+(\epsilon_{12}+\epsilon_{21})^2}$, deviatoric strain
γ	M/N, coordination number ($\gamma \to \gamma_\infty$ at steady-state)
θ_a	second-order principal direction of contact anisotropy (plane systems)
θ_f	second-order principal direction of average normal contact force anisotropy (plane systems)
θ_t	second-order principal direction of average tangential contact force anisotropy (plane systems)
σ, σ_{ij}	stress tensor
σ_n, σ_t	normal and deviatoric invariants of stress tensor
μ	interparticle friction coefficient (i.e., $\mid f_t^c \mid \not> \mu f_n^c$)
v	specific volume

Introduction

It is well known that an understanding of the micromechanical response of granular media is fundamental to the understanding of the macroscopic behavior of these systems during shear deformations. Of primary importance are relationships between the distribution of externally applied forces, which act at the boundaries of a granular assembly, and the microstructure (or fabric) and distribution of interparticle forces that evolves in response to boundary distortions.

Expressions that relate stress as used in continuum mechanics approaches to microfeatures of granular media are unmanageable if discrete information is considered directly. Recently, Rothenburg (1980) and Rothenburg and Bathurst (1989) have proposed a stress-force-fabric relationship for idealized planar assemblies that relates *average* stress in the assembly to fundamental parameters that are explicitly related to statistical *averages* of fabric and interparticle load transmission. The proposed relationship provides a clear link between shear-induced fabric anisotropy and average stress in planar granular assemblies.

The current study shows that for two-dimensional systems the contributions to average stress tensor can be equated directly to invariant quantities associated with a fabric tensor $\boldsymbol{R}$ and two force tensors $\boldsymbol{N}$ and $\boldsymbol{T}$ describing the distribution of average normal and tangential contact forces in the assemblies.

Unfortunately, physical data reported in the literature is incomplete from the point of view of verification of stress–force–fabric relationships proposed in earlier work by the authors. In order to assess the accuracy of the proposed relationships, the results of numerical simulation of assemblies of 1000 discs subjected to shearing deformations are used. The influence of micromechanical properties on macroscopic behavior and the magnitude of coefficients describing anisotropy in these systems is explored. Finally, the paper presents the empirical observation that the steady-state mobilized angle of friction ϕ_∞ is related to fabric anisotropy in the assembly according to the relationship $\sin \phi_\infty = \mu_0 a_\infty$. Here, the coefficient a_∞ is a direct measure of limiting fabric anisotropy at large strain and it is equal to a deviatoric invariant quantity of the fabric tensor $\boldsymbol{R}$ at steady-state (i.e. at constant volume). Furthermore, it is shown that the limiting value of the coefficient of proportionality μ_0 is essentially independent of the magnitude of interparticle frictional capacity and interparticle stiffness.

Theoretical background

Discrete quantities of interest at the micromechanical level of description are illustrated in Fig. 1. Interparticle load transfer between particles can be described by a contact force $\boldsymbol{f}^c$ when particles interact through point contacts. Anisotropy in microstructure (fabric) can be related to statistical distributions of quantities $\boldsymbol{n}^c$ and $\boldsymbol{l}^c$ denoting the unit vector orthogonal to the contact tangent plane (*contact normal*) and a *contact vector* describing the line drawn from the centroid of a contacting particle and the contact point (Rothenburg and Selvadurai, 1981). In this scheme every physical contact contributes two contacts to the system and a vector pair $\boldsymbol{n}^c$, $\boldsymbol{l}^c$ and $\boldsymbol{f}^c$. The

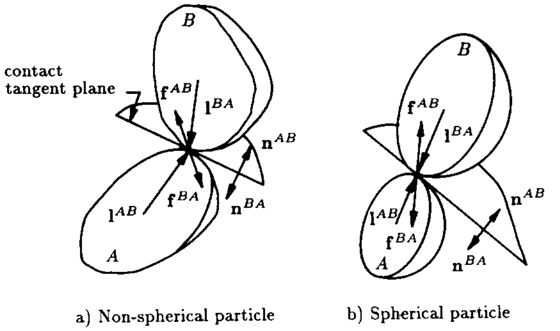

Fig. 1. Contact normals, contact vectors and contact forces.

density of particle packing can be related to *average coordination number* defined as $\gamma = M/N$ where M is the total number of contacts and N is the number of particles comprising the sample volume.

The *average* stress tensor acting through a granular assembly can be explicitly described in terms of quantities $\boldsymbol{f}^c$ and $\boldsymbol{l}^c$ according to:

$$\sigma_{ij} = \frac{1}{V} \sum_{c \in V} f_i^c l_j^c \quad i,\ j = 1, 2, 3 \tag{1}$$

Term V in this expression represents the volume of the system. Expression (1) can be determined from conditions of static equilibrium in these systems and has been reported elsewhere (e.g., Weber (1966), Dantu (1968), Rothenburg (1980) and Christoffersen et al. (1981) amongst others).

Analytical developments are greatly facilitated if spatially homogeneous assemblies comprising a very large number of contacts and particles are considered. If this is done, then discrete quantities in (1) can be replaced by certain continuous distributions. For example, the distribution of contact normal orientations can be described by a function $E(\boldsymbol{n})$ such that the fraction of all assembly contact normals falling within the orientation interval $\mathrm{d}\boldsymbol{n}$ is $E(\boldsymbol{n})\ \mathrm{d}\boldsymbol{n}$ (e.g., Horne 1965). Similarly, distributions describing the distribution of *average* forces $\bar{f}_i(\boldsymbol{n})$ and *average* contact vector lengths $\bar{l}_j(\boldsymbol{n})$ can be used in expression (1) provided that they are uncorrelated with $E(\boldsymbol{n})$. If this is done and an infinite assembly is considered, then expression (1) can be approximated by:

$$\sigma_{ij} = m_v \int_V \bar{f}_i(\boldsymbol{n}) \bar{l}_j(\boldsymbol{n}) E(\boldsymbol{n})\ \mathrm{d}\boldsymbol{n} \tag{2}$$

Term $m_v = M/V$ above denotes *contact density.* Expression (2) was originally reported by Rothenburg (1980) and can also be recovered from general expressions reported by Mehrabadi et al. (1982). For a granular assembly comprising spherical or near-spherical particles and a narrow size-distribution the above expression can be simplified to:

$$\sigma_{ij} = m_v \bar{l}_0 \int_V \bar{f}_i(\boldsymbol{n}) n_j E(\boldsymbol{n})\ \mathrm{d}\boldsymbol{n} \tag{3}$$

where $\bar{l}(\boldsymbol{n}) = \bar{l}_0 \approx \bar{r}_0$. For assemblies comprising spherical particles with a narrow size range, contact density can be equated to coordination number using:

$$m_v = \frac{3\gamma}{4\pi \bar{l}_0^3 v} \tag{4}$$

Here, v denotes assembly specific volume.

Fabric description

The normalized distribution of contacts in granular systems can be described by a three-dimensional symmetric second-order *fabric* tensor $\boldsymbol{R}$. Components of the tensor can be calculated on the basis of discrete information using:

$$R_{ij} = \frac{1}{V} \sum_{c \in V} n_i n_j \tag{5}$$

An equivalent expression for infinite assemblies is:

$$R_{ij} = m_v \int_V E(\boldsymbol{n}) n_i n_j\ \mathrm{d}\boldsymbol{n} \tag{6}$$

Similar quantities have been proposed by Satake (1978), Oda et al. (1982), Mehrabadi et al. (1982) and Kanatani (1984) to describe contact distribution data in granular systems. It is convenient to consider expressions for $E(\boldsymbol{n})$ which can be visualized as three-dimensional surfaces with certain axes of symmetry. The general form of these expressions is:

$$E(\boldsymbol{n}) = \frac{1}{4\pi}\{1 + a_{ij}n_in_j\}, \quad a_{ij} = a_{ji}, \quad a_{kk} = 0 \tag{7}$$

Coefficient terms in (7) have important physical meaning since they can be equated directly to the assembly *fabric* tensor $\boldsymbol{R}$. For an isotropic assembly, coefficient terms are zero and $E(\boldsymbol{n}) = 1/4\pi$. Coefficient terms a_{ij} can be calculated directly from measured data using relationships (5), (6) and (7).

Two-dimensional granular systems

Despite the simplifications introduced above for assemblies of spherical or near-spherical particles, very little data for measured fabric is available in the literature and none for the distribution of average force $\bar{f}_i(\boldsymbol{n})$. However, the stress relationships (2), (3) and fabric expressions (5), (6) and (7) have a two-dimensional analogue (e.g., Rothenburg and Bathurst, 1989). Specifically, the stress relationship (3) for circular or near-circular particle assemblies with a narrow size-distribution becomes:

$$\sigma_{ij} = m_v\bar{l}_0\int_0^{2\pi}\bar{f}_i(\theta)n_jE(\theta)\,\mathrm{d}\theta \quad i,\ j = 1, 2 \tag{8}$$

Similarly, the distribution of contact normal orientations is:

$$E(\theta) = \frac{1}{2\pi}\{1 + a_{ij}n_in_j\}, \quad a_{ij} = a_{ji}, \quad a_{kk} = 0 \tag{9}$$

Here $\boldsymbol{n} = (\cos\theta, \sin\theta)$. Equivalently, $E(\theta)$ can be expressed as a Fourier series. If fourth-order contact fabric is also included then the following Fourier series expression can be used to describe fabric in these systems (Rothenburg, 1980):

$$E(\theta) = \frac{1}{2\pi}\{1 + a\cos 2(\theta - \theta_a) + b\cos 4(\theta - \theta_b)\} \tag{10}$$

Coefficients a and b are invariant quantities describing second and fourth-order anisotropy in the distribution of contact normal orientations. Terms θ_a and θ_b represent principal directions of contact normal anisotropy. The value of the coefficient term a is a deviatoric invariant quantity of the second-order fabric tensor $\boldsymbol{R}$ and θ_a is an eigenvector of this tensor. Coefficient a and the principal direction θ_a can be determined from discrete data by equating $E(\theta)$ to the fabric tensor $\boldsymbol{R}$ as outlined in the previous section. Similar relationships exist between the fourth-order term b and θ_b in expression (10) and a symmetric fourth-order fabric tensor. However, detailed analysis of data from experiments on assemblies of photo-elastic discs reported by Konishi (1978) showed that no improvement in fit was achieved by considering terms higher than fourth-order in expression (10) (Bathurst, 1985).

The average contact force acting at contacts with orientation θ can be decomposed into an average *normal* force component $\bar{f}_n(\theta)$ and an average *tangential* (or shear) force component $\bar{f}_t(\theta)$ (e.g., Rothenburg and Selvadurai, 1981, 1985). Hence:

$$\bar{f}_i(\theta) = \bar{f}_n(\theta)n_i + \bar{f}_t(\theta)t_i \tag{11}$$

If this is done then expression (8) can be rewritten as:

$$\sigma_{ij} = m_v\bar{l}_0\int_0^{2\pi}\{\bar{f}_n(\theta)n_in_j + \bar{f}_t(\theta)t_in_j\}E(\theta)\,\mathrm{d}\theta \tag{12}$$

Here $\boldsymbol{t} = (-\sin\theta, \cos\theta)$ and represents directions orthogonal to $\boldsymbol{n}$. Rothenburg (1980) has proposed that distributions for *average* contact force components in two-dimensional particulate systems may be represented by Fourier series expressions of the form:

$$\begin{aligned}\bar{f}_n(\theta) &= \bar{f}_0\{1 + a_n\cos 2(\theta - \theta_f)\}\\ \bar{f}_t(\theta) &= \bar{f}_0\{a_\omega - a_t\sin 2(\theta - \theta_t)\}\end{aligned} \tag{13}$$

For isotropic assemblies, $\bar{f}_0$ is a constant representing the average normal force over all contacts in the assembly. For anisotropic assemblies, where the number of contacts in different orientations varies, $\bar{f}_0$ is the measure of average normal contact force when all groups are given equal weight, i.e.:

$$\bar{f}_0 = \int_0^{2\pi} \bar{f}_n(\theta)\, d\theta \tag{14}$$

Terms a_n, a_ω and a_t are non-dimensional *coefficients of contact force anisotropy*. Similar to θ_a and θ_b in eqn. (10), terms θ_f and θ_t represent preferred directions for contact force distributions and are called major principal *directions of contact force anisotropy*. Moment equilibrium for these systems requires that:

$$\int_0^{2\pi} \bar{f}_t(\theta) E(\theta)\, d\theta = 0 \tag{15}$$

The constant term a_ω in expression (13) for $\bar{f}_t(\theta)$ is required to satisfy the general case of non-coincidence of tangential contact force anisotropy and anisotropy in contact normals. Physically, non-zero values of a_ω correspond to a situation in which a non-symmetrical distribution of shear contact forces is required to compensate for a lack of contact normals in the direction of maximum loading.

Similar to the relationship between $E(\theta)$ and fabric tensor $\boldsymbol{R}$, the distributions for average force components $\bar{f}_n(\theta)$ and $\bar{f}_t(\theta)$ can be equated to average normal and average tangential contact force tensors $\boldsymbol{N}$ and $\boldsymbol{T}$. Here $\boldsymbol{T}$ is a deviator tensor. Again, coefficient terms are invariant quantities of these tensors and directions of anisotropy are principal directions (eigenvectors) of these tensors. Hence, these quantities can be determined using the following approximations:

$$\begin{aligned} N_{ij} &= \frac{1}{2\pi}\int_0^{2\pi} \bar{f}_n(\theta) n_i n_j\, d\theta \approx \frac{1}{N_g}\sum_{\theta_g} \bar{f}_n^c n_i n_j \\ T_{ij} &= \frac{1}{2\pi}\int_0^{2\pi} \bar{f}_t(\theta) t_i n_j\, d\theta \approx \frac{1}{N_g}\sum_{\theta_g} \bar{f}_t^c t_i n_j \end{aligned} \tag{16}$$

The term N_g represents the number of orientation intervals used in the approximation and θ_g the group orientation.

Stress–Force–Fabric relationship for plane systems

If directions of anisotropy in equations (10) and (13) are coincident (i.e., $\theta_a = \theta_f = \theta_t$) and fourth-order terms in (10) are neglected then integration leads to average stress components expressed as:

$$\begin{aligned} \sigma_{11} &= p\left\{1 + \frac{aa_n}{2} + \tfrac{1}{2}(a + a_n + a_t)\cos(2\theta_a)\right\} \\ \sigma_{22} &= p\left\{1 + \frac{aa_n}{2} - \tfrac{1}{2}(a + a_n + a_t)\cos(2\theta_a)\right\} \\ \sigma_{12} &= \sigma_{21} = p\left\{\tfrac{1}{2}(a + a_n + a_t)\sin(2\theta_a)\right\} \end{aligned} \tag{17}$$

where:

$$p = \frac{m_v \bar{l}_0 \bar{f}_0}{2} \tag{18}$$

Invariants of the average stress tensor in the form of parameters of the Mohr circle of stress are as follows:

$$\sigma_n = \frac{\sigma_{11} + \sigma_{22}}{2} = p\left(1 + \frac{aa_n}{2}\right) \tag{19}$$

$$\sigma_t = \sqrt{\left(\frac{\sigma_{11} - \sigma_{22}}{2}\right)^2 + \sigma_{12}^2} = \frac{p}{4}(a + a_n + a_t) \tag{20}$$

The ratio of the above two invariants is independent of the number of contacts and is as follows:

$$\frac{\sigma_t}{\sigma_n} = \frac{\tfrac{1}{2}(a + a_n + a_t)}{\left(1 + \frac{a_n a}{2}\right)} \tag{21}$$

The latter quantity is frequently associated with the mobilized angle of friction for cohesionless material (i.e., $\sin\phi = \sigma_t/\sigma_n$). Note however, that the derived relationships are for any plane granular assembly of discs, irrespective of specific types of particle interactions. This relationship relates characteristics of microstructural response with the level of deviatoric load. For brevity, expression (21) can be referred to as the stress–force–fabric relationship. Analysis of physical data reported in the literature shows that coefficient terms a, a_n are small for circular particles and hence no significant loss in accuracy results if product terms are neglected. If this is done the following conceptually simple relationship emerges:

$$\frac{\sigma_t}{\sigma_n} = \frac{1}{2}(a + a_n + a_t) \tag{22}$$

Expression (22) was originally reported by Rothenburg (1980) and verified on the basis of numerical simulation of a biaxial compression test reported by Bathurst (1985) and Rothenburg and Bathurst (1989). This expression reveals that for the planar assemblies under study the shear capacity of the system is directly proportional to the sum of contributing anisotropy in contact normals (i.e., fabric) and anisotropy in the distribution of average normal and average tangential contact forces that evolves in response to deviatoric load. The current paper extends the earlier work by the authors to examine the influence of the magnitude of micromechanical properties on the relative contributions of coefficients of anisotropy to assembly shear capacity and explores empirically observed relationships between components of system anisotropy.

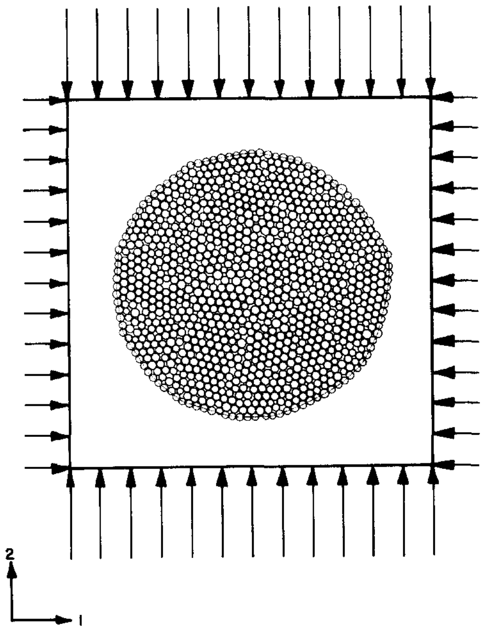

Fig. 2. A 1000 disc assembly.

Numerical simulation of planar assemblies of discs

General

Numerical experiments in this study were originally described by Bathurst (1985) and were carried out on assemblies comprising 1000 discs such as that shown on Fig. 2. The test assemblies were subjected to different load paths by applying boundary forces to perimeter discs corresponding to a prescribed average stress field. The simulations were carried out using a computer program called DISC. The program implements an explicit time-finite-difference scheme which solves the system of equations modelling a dynamic transient mechanical system. The loading rate and damping parameters are selected such that inertial forces in these numerical experiments are negligibly small. The finite-difference scheme is identical to that reported by Cundall and Strack (1979) and has also been used in similar numerical simulations reported by the authors for assemblies of bonded discs (Bathurst and Rothenburg, 1988a,b).

Contact force–displacement relationships

In the current study, the particles are assumed to transmit force through compliant point contacts that interact according to a no-tension elastic–plastic Coulomb friction law. Over the elastic range the contacts are assumed to interact linearly as follows:

$$f_\mathrm{n}^c = k_\mathrm{n}\frac{\Delta_\mathrm{n}^c}{l} \qquad f_\mathrm{t}^c = k_\mathrm{t}\frac{\Delta_\mathrm{t}^c}{l} \tag{23}$$

Here term Δ_n^c is the normal displacement at a physical contact which is measured with respect to the change in length between particle centers located a distance l apart. Term Δ_t^c refers to tangential (shear) contact displacements. Parameters k_n and k_t are normal and tangential interparticle stiffnesses and in this paper are assigned magnitudes such that $k_\mathrm{n}/k_\mathrm{t} = 1$ for all particles. Interparticle shear forces are restricted by a Coulomb-type friction law such that:

$$| f_\mathrm{t}^c | \ngtr f_\mathrm{n}^c \mu \tag{24}$$

where μ represents the interparticle friction coefficient. For comparison purposes all particle contacts in an assembly were assigned constant values of interparticle friction coefficient over the range $0 \leqslant \mu \leqslant 0.5$. Truly elastic particles in three-dimensional assemblies can be expected to interact in a non-linear fashion (Mindlin, 1949). In real systems, non-linear interactions may be due to surface asperities or slight irregularities in particle shape. Nevertheless, a linear model offers simplicity and can provide insight into the link between micromechanical properties and macroscopic behavior. Furthermore, the stress–force–fabric relationships (21) and (22) that are the principal focus of this investigation are independent of the form of the contact model adopted.

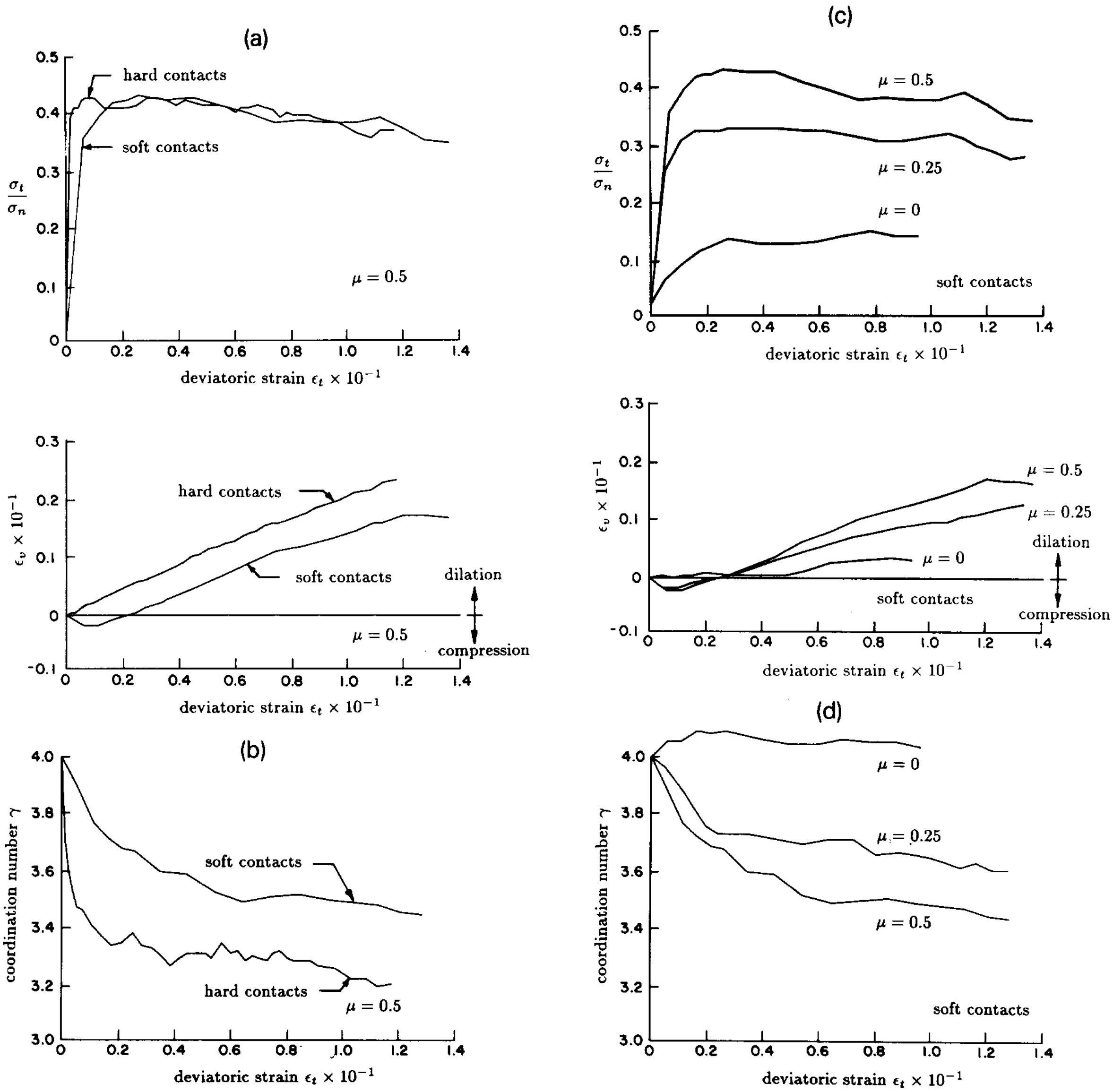

Fig. 3. Results of biaxial compression tests: (a) stress–strain response (variable interparticle stiffness), (b) coordination number (variable interparticle stiffness), (c) stress–strain response (variable interparticle friction coefficient), and (d) coordination number (variable interparticle friction coefficient).

All tests were carried out using an initially dense isotropic assembly (i.e. $a = 0$, $b = 0$ and $\gamma = 4$) made up of 20 different disc radii with a narrow range of particle sizes (i.e. $0.78 \leqslant r/\bar{r}_0 \leqslant 1.29$). The initial assembly was also isotropic with respect to average contact lengths (i.e. $\bar{l}(\theta) = \bar{l}_0 \approx \bar{r}_0$) and this distribution did not change during subsequent shearing deformations. The assemblies were subjected to biaxial compression and pure shear following compaction under the same hydrostatic stress condition. A pure shear test refers to a stress path in σ_t, σ_n space where the initial hydrostatic stress state is maintained constant during boundary shearing deformations. During numerical simulations the direction of maximum principal stress was maintained constant at $\theta_\sigma = \pi/2$ for biaxial compression tests and at $\theta_\sigma = \pi/4$ for pure shear tests.

General behavior

The results of a series of biaxial compression tests are summarized on Fig. 3. The tests were carried out with two different values of interparticle stiffness and three values of interparticle friction coefficient. The following general observations can be made: At low levels of strain the samples were observed to behave in a linear elastic manner and hence the initial bulk and shear moduli of the assemblies were directly controlled by the magnitude of contact stiffness assigned to the particles. After the assemblies became unlocked and relatively mobile under post-peak shear deformations the magnitude of normalized shear capacity and rate of dilatancy appeared to be essentially independent of interparticle stiffness (Fig. 3a). The influence of interparticle friction coefficient (μ) on macroscale behavior can be seen in Fig. 3c. In general, the normalized shear capacity and rate of dilatancy were observed to diminish with decreasing interparticle frictional capacity.

Figures 3b and 3d show the evolution of average coordination number during shearing deformation in these tests. In general the coordination number of the assemblies was seen to decrease with strain and this observation is consistent with sample dilatancy observed at the macroscale. At the beginning of each test the rate at which contacts were lost is large. This initial behavior is due to elastic unloading of the systems prior to the assemblies becoming *unlocked* and does not reflect any significant spatial rearrangement of the particles. The definition of a contact adopted in this investigation is that a contact exists if it transmits load. This definition assures that coordination number is sensitive to elastic unloading. As the interparticle stiffness or friction coefficient was increased the limiting value of coordination number that could be sustained by the assemblies under quasi-static conditions was seen to decrease. From consideration of static equilibrium it can be shown that the minimum admissible value for coordination number γ is 3. In qualitative terms, as interparticle stiffness and interparticle frictional capacity increases the combination of interparticle contact forces available to maintain the assembly in static equilibrium increases and therefore a lower coordination number is possible for a given value of contact anisotropy. As expected, the test results show that in the limit of frictionless particles ($\mu = 0$) the numerical assemblies were non-dilatant and incapable of developing significant fabric anisotropy or reduced coordination number below the initial state.

The end of each test was characterized by a *steady-state* condition in which volumetric strain, density and shear strength became constant. In soil mechanics terminology this condition corresponds to *critical state*. From a micromechanical point of view careful observation of the numerical assemblies at steady-state revealed that at this stage in a test the growth and collapse of predominant load-carrying chains of particles occurred at about the same rate and all statistical parameters describing the intensity of particle packing (e.g. γ, m_v), anisotropy in contact forces (i.e. a_n, a_t) and fabric (i.e. a) remained unchanged.

Figure 4 presents similar data from the results of pure shear tests. A noticeable macroscopic difference in mechanical behavior is that the pure shear tests generally exhibit greater post-peak strain softening than the comparable biaxial compression tests. For the same micromechanical properties the pure shear and biaxial tests reflected characteristics of the macroscopic behavior

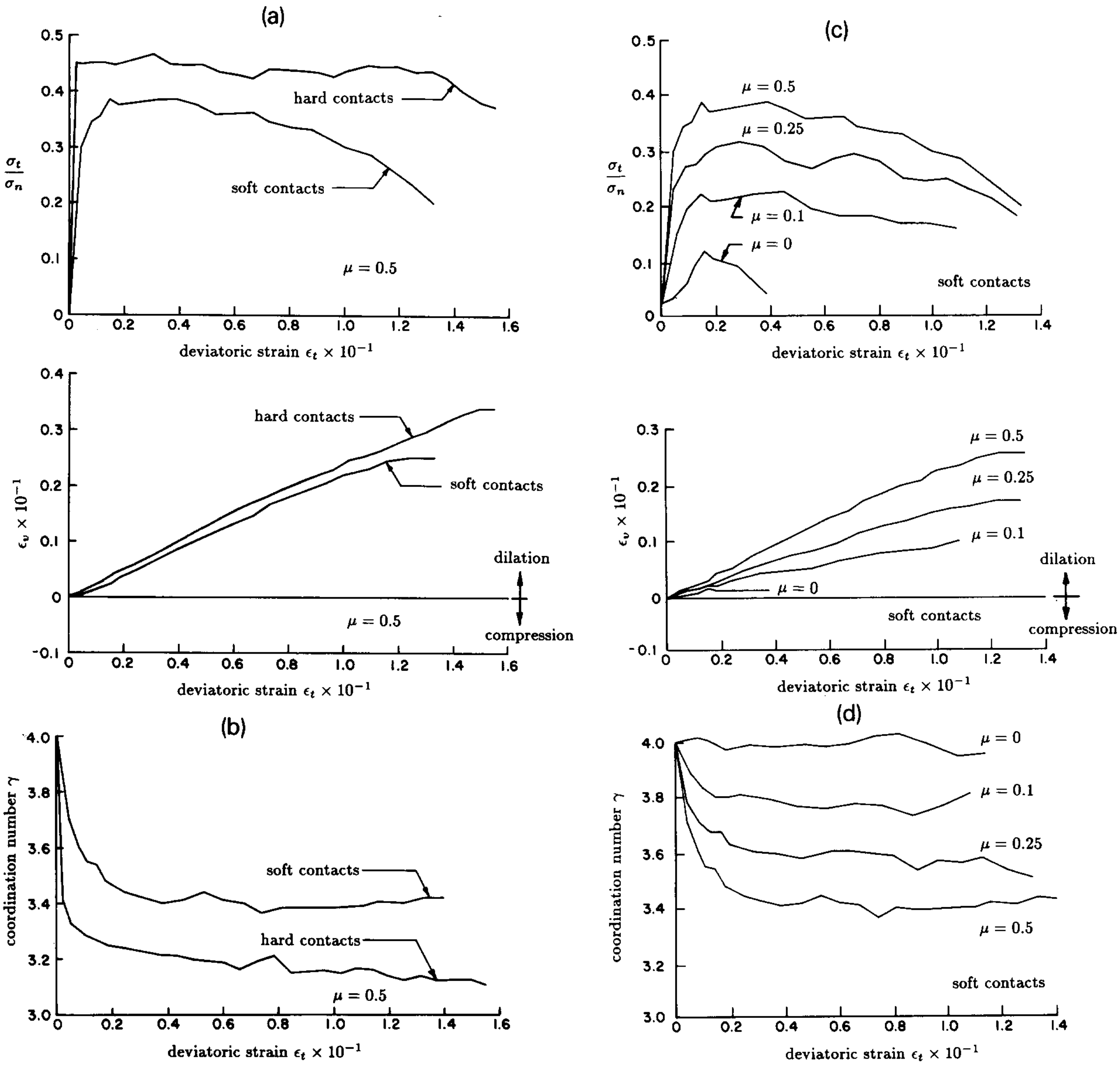

Fig. 4. Results of pure shear tests: (a) stress–strain response (variable interparticle stiffness), (b) coordination number (variable interparticle stiffness), (c) stress–strain response (variable interparticle friction coefficient) and (d) coordination number (variable interparticle friction coefficient).

of many actual granular materials which exhibit dilatancy rate and critical state densities that are suppressed with increasing normal stress.

Evolution of anisotropy in microfeatures

Normalized distributions for contact normals and average interparticle force components with respect to group orientations taken at peak shear strength in a biaxial compression test and pure shear test are illustrated in Figs. 5 and 6. The measured data is presented together with the approximations to the distributions using Fourier series expressions (10) and (13) introduced earlier but limited to second-order terms. The coefficients of anisotropy and directions of anisotropy have been determined using tensorial relationships (6),

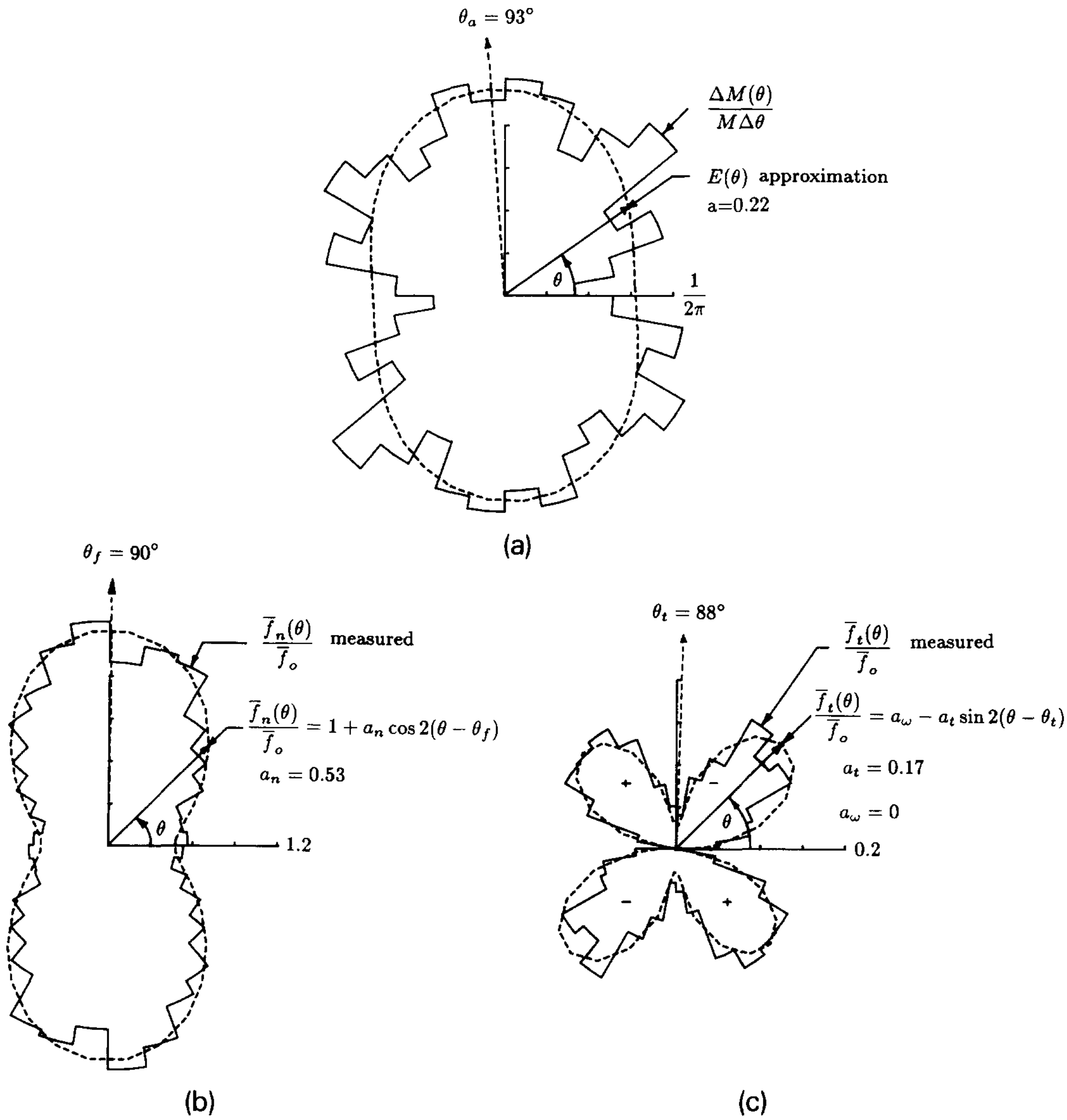

Fig. 5. Distribution of contact normals and average force components at peak shear in biaxial compression test: (a) contact normals, (b) average normal forces, and (c) average tangential (shear) forces.

(16). The figures show that the approximations appear to visually well-represent the measured data. The range of values for coefficients a and a_n calculated from these numerical simulations was similar to that interpreted by Bathurst (1985) from the results of tests on photo-elastic discs reported by Oda and Konishi (1974b) and Konishi (1978). In the current study, it can be seen that directions of anisotropy are essentially coincident with the direction of maximum principal stress. In all tests, regardless of stress path, coincidence of force, fabric and stress tensors was observed at all stages in a test even for assemblies subjected to stress rotations. The explanation for this observation is that normal forces are controlled directly by the average stress tensor in the assembly and since the distribution of contacts is defined by contacts that actively transmit force then the coincidence of

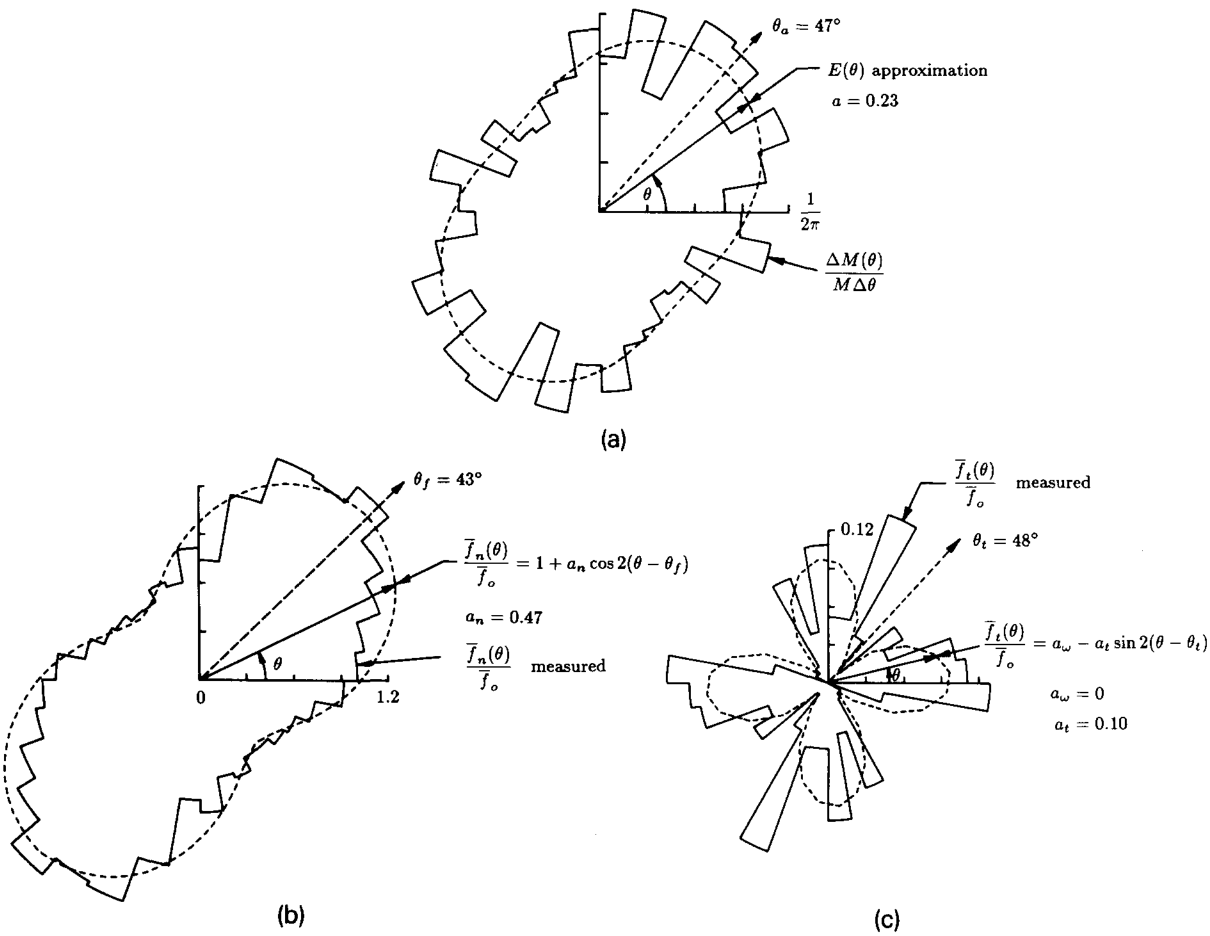

Fig. 6. Distribution of contact normals and average force components at peak shear in pure shear test: (a) contact normals, (b) average normal forces, and (c) average tangential (shear) forces.

stress, force and fabric tensors is assured. The coincidence of contact normal distributions and average shear forces was also reflected in the observation that calculated values for coefficient term a_ω were essentially zero at all stages during shearing deformations. The coincidence of quantities describing the preferred direction of contact normals in photo-elastic disc experiments and the direction of maximum loading has been noted by Oda and Konishi (1974a,b). The results of our tests with frictional contacts have shown that there is a progressive loss in the number of contacts oriented in the direction of minimum principal stress (i.e., the direction of tensile strain) and it is this loss of contacts or *destructuring* in preferred directions that generates fabric anisotropy in these systems. This phenomenon has been noted in both physical experiments and in previous numerical simulations reported by the authors and others (e.g., Oda and Konishi, 1974a; Cundall et al., 1982, Rothenburg and Bathurst, 1989).

Verification of stress-force-fabric relationship

Figures 7a and 7b show the evolution of coefficients of anisotropy a, a_n and a_t describing the intensity of anisotropy in fabric (contact normals) and average force components during biaxial compression and pure shear. In general the tests show that the maximum value of normal contact force

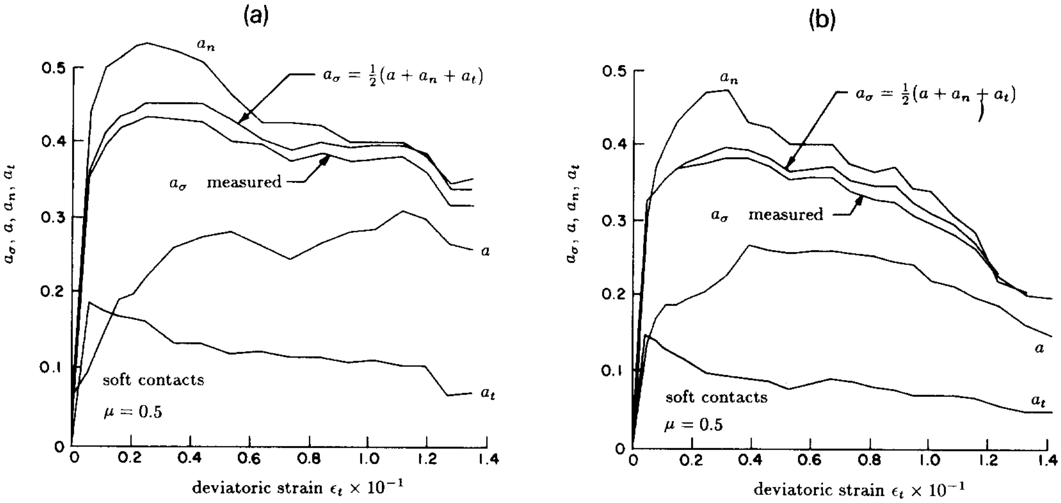

Fig. 7. Invariant stress ratio and coefficients of anisotropy during shear deformations: (a) biaxial compression test, and (b) pure shear test.

anisotropy occurred at about the same point in the test as the measured peak shearing resistance but diminished thereafter. The magnitude of anisotropy in tangential contact forces a_t was significantly lower than a_n over the course of each test and was seen to increase rapidly during elastic compression but to diminish steadily as the system became unlocked and particle mobility increased. During the biaxial compression test a constant level of contact normal anisotropy was sustained during sample dilation as a consequence of the progressively higher level of average normal stress. A similar sustained level of contact normal anisotropy can be interpreted from data reported by Biarez and Wiendiek (1963) from biaxial compression tests carried out on assemblies of planar particles. By comparison, the pure shear test in this investigation exhibited diminishing fabric anisotropy as the sample approached steady-state.

Superimposed on the figures are measured values of invariant stress ratio $a_\sigma = \sigma_t/\sigma_n$ and theoretical approximations to these curves using expression (22). The approximations and measured values for normalized shear capacity are very close. It should be noted that the difference in the curves would virtually disappear if the full expression for the invariant stress ratio was used (i.e. eqn. (21)). Similar accuracy has been reported by Bathurst (1985) for tests having a wide range of interparticle properties and subjected to a variety of stress paths. It appears from Fig. 7 that the major contribution to mobilized shear strength in these assemblies at all strain levels is due to anisotropy in normal contact forces plus stress-induced anisotropy in fabric (contact normals). The direct contribution of interparticle shear force during shear deformations can be seen to vary from about 25% during initial elastic deformation of the samples to about 11% of the total capacity of the assemblies at steady-state.

The relative values of a_n and a_t confirm the visual impressions reported in an earlier paper by the authors (Rothenburg and Bathurst, 1989) that load transfer is largely due to interparticle forces that act normal to the contact plane. Detailed measurements of the mobilized interparticle shear capacity showed that even in directions with peak tangential shear force $\bar{f}_t(\theta)$ the mobilized coefficient of friction was never greater than 30% of interparticle frictional capacity. The absence of fully-mobilized friction in sheared two-dimensional assemblies of discs has been noted by Oda and Konishi (1974a) from the results of physical experiments with photo-elastic discs. A conspicuous absence of oblique contact forces between discs is also apparent from similar physical experiments reported by De Josselin De Jong and Verruijt (1969).

Influence of interparticle properties on anisotropy components

Figures 8 and 9 summarize peak and steady-state values of coefficient terms a, a_n, a_t and normalized shear strength a_σ determined from the results of numerical simulations on discs having a range of interparticle friction coefficient μ. A comparison of the data shows that generally higher

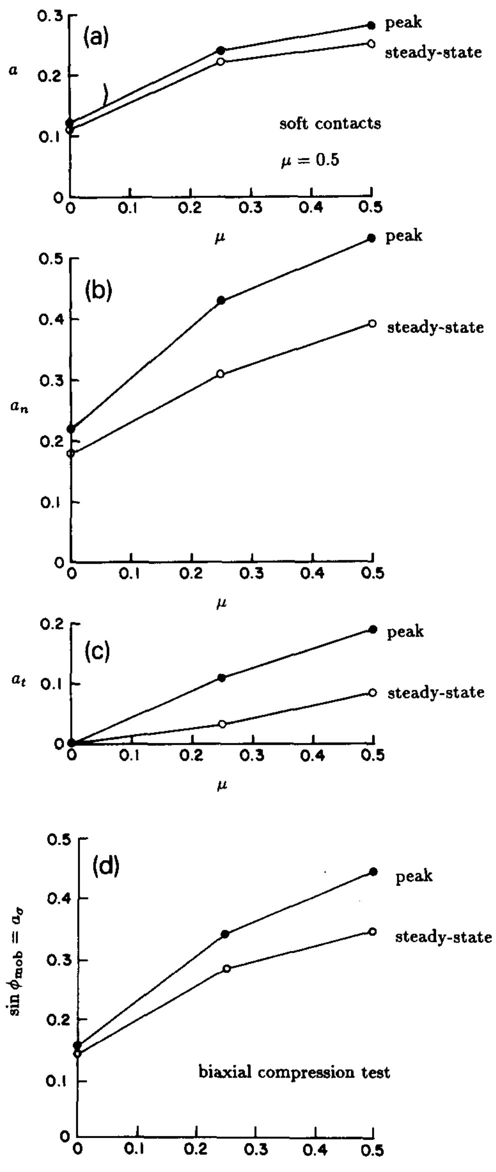

Fig. 8. Influence of interparticle friction coefficient on coefficients of anisotropy and mobilized friction angle during biaxial compression test: (a) contact normal anisotropy, (b) average normal force anisotropy, (c) tangential (shear) force anisotropy, and (d) mobilized angle of friction.

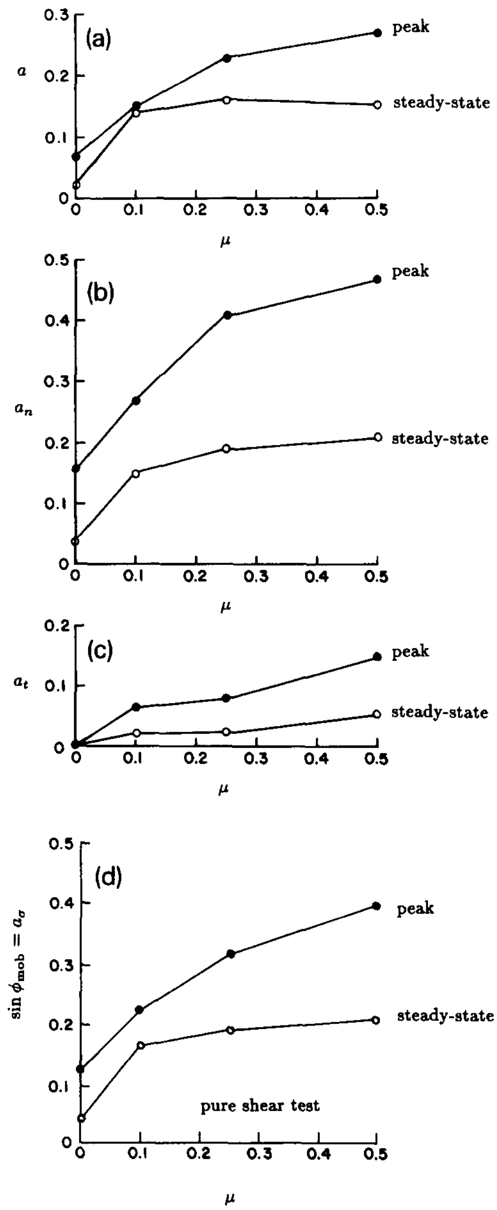

Fig. 9. Influence of interparticle friction coefficient on coefficients of anisotropy and mobilized friction angle during pure shear test: (a) contact normal anisotropy, (b) average normal force anisotropy, (c) tangential (shear) force anisotropy, and (d) mobilized angle of friction.

coefficient values were observed during the biaxial compression test as compared to the pure shear test. This difference indicates that anisotropy in these systems is sensitive to the magnitude of average confining stress. As σ_n increased, the assemblies under investigation were better able to sustain higher levels of anisotropy in fabric and force components. Comparison of mobilized friction angle reveals that for the assemblies subjected to pure shear the steady-state value of mobilized friction angle ϕ_{mob} was essentially independent of interparticle friction coefficient for (say) $\mu > 0.1$. This observation supports in part the somewhat controversial observation advanced by Skinner (1969) that under shearing deformations at constant confining pressure the macroscopic shearing resistance of ballotini is independent of interparticle friction angle. Careful analysis of mobilized interparticle shear capacity in numerical simulations showed that a small portion of the available shear capacity was mobilized at peak and steady-state. This observation is supported by direct measurement of mobilized friction angle reported by Oda and Konishi (1974a) for assemblies of photo-elastic discs and explains the generally non-linear relationship between the interparticle friction coefficient and macroscopic shear capacity in both series of tests. The micromechanical explanation for this phenomenon is that only a finite portion of interparticle shear force capacity is required to develop the limiting values of anisotropy in fabric and normal contact forces observed at steady-state. Large interparticle shear capacity, even if available, is not mobilized in these systems at large strain since the constituent discs have great rotational freedom due to low contact density and will shed high tangential contact forces as soon as they develop. A qualitative explanation of the indirect contribution of interparticle shear capacity to system shear capacity can be made by imagining the assembly as comprising chains of load bearing *columns*. The contribution of interparticle shear capacity is related to the lateral support available to these columns.

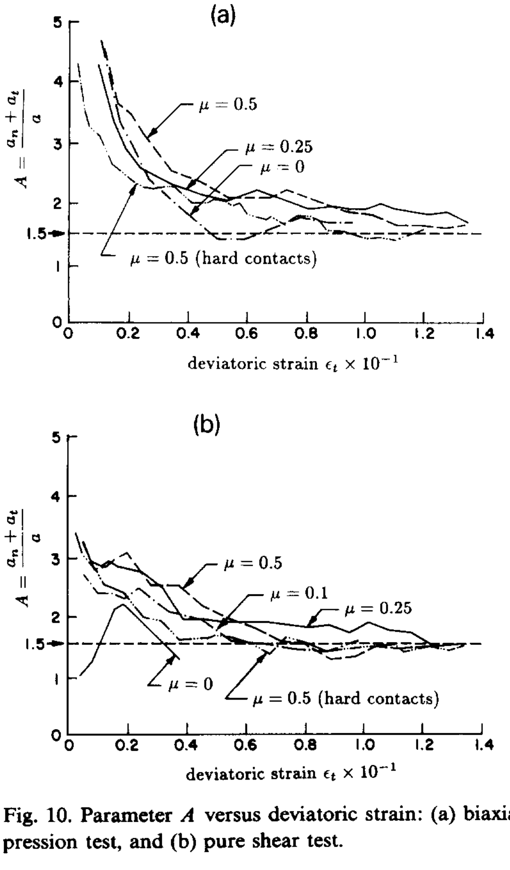

Fig. 10. Parameter A versus deviatoric strain: (a) biaxial compression test, and (b) pure shear test.

Relationship between parameters of fabric and force anisotropy

Figure 10 plots the ratio $A = (a_n + a_t)/a$ for several tests having a range of interparticle properties. This data together with the measured reduction in coordination number recorded during shear suggests that

$$A \to 1.5 \quad \text{for } \gamma \to \gamma_\infty$$

regardless of interparticle stiffness, coefficient of friction and stress path for the assemblies under study. Here γ_∞ is equivalent to critical state in soil mechanics terminology. In terms of mobilized frictional capacity this observation together with the stress-force-fabric relationship (22) leads to the general expression:

$$\sin \phi_\infty = \mu_0 a_\infty \text{ where } \mu_0 = \left(\frac{1+A}{2}\right) \tag{25}$$

It can be easily seen that for these assemblies the coefficient of proportionality μ_0 has a value of

1.25 at steady-state. Rothenburg et al. (1989) have recently proposed that the quantity μ_0 represents an energy dissipation constant that is an important part of a simplified micromechanics-based constitutive model for planar assemblies.

Concluding remarks

The information presented in the paper emphasizes the fact that shear strength of granular materials depends on the ability of the assembly to develop anisotropy in contact orientations. The outlined theoretical developments and results of numerical experiments on plane granular assemblies show that there is an explicit link between the angle of friction at large strain and a parameter describing the limiting degree of anisotropy.

Most theoretical results presented in the paper are for the special case of plane assemblies of particles although the general expression for the stress tensor is equally valid for 3D assemblies of arbitrary shaped particles. Limited data on the development of anisotropy in sands indicate trends similar to plane assemblies although the degree of anisotropy in 3D assemblies appears to be much higher (Bathurst, 1985).

References

Bathurst, R.J. (1985), A study of stress and anisotropy in idealized granular assemblies, Ph.D. Dissertation, Queen's University at Kingston, Ontario, Canada.

Bathurst, R.J., and L. Rothenburg (1988a), Micromechanical aspects of isotropic granular assemblies with linear contact interactions, *J. Appl. Mech. ASME 55,* 17.

Bathurst, R.J., and L. Rothenburg (1988b), Note on a random isotropic granular material with negative Poisson's ratio, *Int. J. Eng. Sci. 26* (4), 373.

Biarez, J. and K. Wiendieck (1963), La comparaison qualitative entre l'anisotropie mécanique et l'anisotropie de structure des milieux pulvérulents, *Acad. Sci. C. R. 256,* 1217.

Christoffersen, J., M.M. Mehrabadi and S. Nemat-Nasser (1981), A micromechanical description of granular material behaviour, *J. Appl. Mech. Trans. ASME 48,* 339.

Cundall, P.A. and O.D.L. Strack (1979), A discrete numerical model for granular assemblies, *Géotechnique 29* (1), 47.

Cundall, P.A., A. Drescher and O.D.L. Strack (1982), Numerical experiments on granular assemblies; Measurements and observations, IUTAM Conf. Deformation and Failure of Granular Materials, Delft, A.A. Balkema, Rotterdam, p. 355.

Dantu, P. (1968), Étude statistique des forces intergranulaires dans un milieu pulvérulent, *Géotechnique 18* (1), 50–55.

De Josselin de Jong, G. and A. Verruijt (1969), Etude photoelastique d'un empilement de disques, *Can. Grpe Etude. Rheol. 2,* 73–86.

Horne, M.R. (1965), The behaviour of an assembly of rotund, rigid, cohesionless particles I & II, *Proc. R. Soc. London 286,* 62.

Kanatani, K. (1984), Distribution of directional data and fabric tensors, *Int. J. Eng. Sci., 22* (2), 149–164.

Konishi, J. (1978), Microscopic model studies on the mechanical behaviour of granular materials, in: S.C. Cowin and M. Satake, eds., Proc. U.S.–Japan Seminar on Continuum-Mechanical and Statistical Approaches in the Mechanics of Granular Materials, Tokyo, Gakujutsu Bunken Fukyukai, Tokyo, Japan, p. 27.

Mehrabadi, M.M., S. Nemat-Nasser and M. Oda (1982), On statistical description of stress and fabric in granular materials, *Int. J. Num. Anal. Meth. Geomech. 6,* 95.

Mindlin, R.D. (1949), Compliance of elastic bodies in contact, *J. Appl. Mech. ASME 16,* 259.

Oda, M. (1972), The mechanism of fabric changes during compressional deformation of sand, *Jpn. Soc. Soil Mech. Found, Eng. 12* (2) 1.

Oda, M. and J. Konishi (1974a), Microscopic deformation mechanism of granular material in simple shear, *Jpn. Soc. Soil Mech. Found. Eng. 14* (4) 25.

Oda, M. and J. Konishi (1974b), Rotation of principal stresses in granular material in simple shear, *Jpn. Soc. Soil Mech. Found. Eng. 14* (4) 39.

Oda, M., S. Nemat-Nasser and M.M. Mehrabadi (1982), A statistical study of fabric in a random assembly of spherical granules, *Int. J. Num. Anal. Meth. Geomech. 6,* 77.

Rothenburg, L. (1980), Micromechanics of idealized granular systems, Ph.D. Dissertation, Carleton University, Ottawa, Ontario, Canada.

Rothenburg, L., and R.J. Bathurst (1989), Analytical study of induced anisotropy in idealized granular materials, *Géotechnique 39* (4), 601.

Rothenburg, L., and A.P.S. Selvadurai (1981), A micromechanical definition of the Cauchy stress tensor for particulate media, in: A.P.S. Selvadurai, ed., Proc. Int. Symp. on the Mechanical Behaviour of Structured Media, Ottawa, Ontario, Canada. Elsevier, Amsterdam.

Rothenburg, L., and A.P.S. Selvadurai (1985), Anisotropic fabric of plane granular assemblies and elements of their mechanical response, in: J.-P. Boehler, ed., *Plastic Behavior of Anisotropic Solids,* Proc. CNRS International Colloquium 319, 1981, Éditions du Centre National de la Recherche Scientifique, Paris, p. 29.

Rothenburg, L., R.J. Bathurst and E.L. Matyas (1989), Mechanisms of fabric evolution in granular media, In: Proc. 12th Conference Int. Soc. for Soil Mech. and Found. Eng., Rio de Janeiro, Brazil, A.A. Balkema, Rotterdam.

Satake, M. (1978), Constitution of mechanics of granular materials through the graph theory, in: S.C. Cowin and M. Satake, eds., Proc. U.S.–Japan Seminar on Continuum-Mechanical and Statistical Approaches in the Mechanics of Granular Materials, Tokyo, Gakujutsu Bunken Fukyukai, Tokyo, Japan,, p. 47.

Skinner, A.E. (1969), A note on the influence of interparticle friction on the shearing strength of a random assembly of spherical particles, *Géotechnique 19* (1), 150.

Weber, J. (1966), Recherches concernant les contraintes intergranulaires dans les milieux pulvérulents, *Bull. de Liaison Ponts et Chaussées 20*, 3–1.